Determination of Dynamic Parameters Controlling Atomic Scale Etching of Si(100)-(2 × 1) by Chlorine

M. Chander, D. A. Goetsch, C. M. Aldao,* and J. H. Weaver

Department of Materials Science and Chemical Engineering, University of Minnesota, Minneapolis, Minnesota 55455

(Received 7 October 1994)

Scanning tunneling microscopy shows that Cl-induced pitting of Si(100)-(2 × 1) is initiated by the creation of single dimer vacancies on terraces. These pits grow laterally by dimer removal either along the dimer row or from an adjacent row. Quantitative analysis of the vacancy size distribution shows that the rate constant for linear growth is 4.7 ± 1 times that for branch creation at 850 K. This indicates that the difference in dimer removal energy in these two directions is 0.11 ± 0.02 eV, a difference that accounts for the observed surface morphologies.

PACS numbers: 61.16.Ch, 61.72.Ef, 81.60.Cp

Etch products and overall etch rates have been established for Si(100) for spontaneous etching with halogens based on analyses of the species liberated from the surface [1–4]. Recently, scanning tunneling microscopy has provided atomic level insight into structural changes on Si(100) that accompany spontaneous etching under model conditions [5–8]. A critical point that has not been addressed is whether etching pathways involving atomic level interactions could be determined so that information about the process dynamics could be extracted. The purpose of this paper is to show that etch pit growth can be quantified, that the size distribution and shape anisotropy of the pits can be deduced, and that activation energies for Si removal along and perpendicular to the dimer row direction can be determined. The implication is that the prediction of atomic details is possible for surfaces exposed to halogens, a capability that can be extended to other systems through the application of the protocol established here [9].

Since surface diffusion barriers are typically much smaller than desorption activation energies, the rate limiting process for etching is the desorption of volatile molecules, not the transport of etchant atoms to pit edges. Pit growth, then, can be understood as a function of desorption activation energies that reflect interactions between neighboring atoms. For a system like Cl-Si(100)-(2 × 1), however, it is possible that the etching phenomena would be too complicated for simple analysis, or the involved energies for the different processes would be too similar, giving rise to random pit distributions. From analysis of postetch scanning tunneling microscopy (STM) images, we found that this is not the case. Instead, our data exhibit a definite pattern that allows insight into mechanisms of pit formation and growth, as well as step etching. Pits are found to be highly asymmetric, longer in the dimer row direction, with areal densities following distinct distributions.

The STM experiments were conducted using a Park Scientific microscope in a chamber with a base pressure of 8×10^{-11} Torr. Si wafers, oriented within 0.2° of (100), were degassed overnight at 600 °C and flash heated to 1200 °C to produce ordered Si(100)-(2 × 1) with defect densities of 2%–3% [10,11]. An electrochemical cell was used to provide Cl_2 at a constant flux, with the current through the cell serving as a direct measure of the Cl_2 release [5]. Under our experimental conditions, a fluence from the source of 2 mA s produces approximately one monolayer (ML) of Cl on Si(100) at 300 K where 1 ML = 6.98×10^{14} atoms cm^{-2}. In all cases, the sample was maintained at 850 K during Cl_2 exposure. The samples were cooled rapidly to room temperature immediately after shutting off the Cl_2 source. STM imaging was done in the constant current mode [7].

Figure 1 shows an STM image of Si(100)-(2 × 1) obtained after exposure to 9.6 mA s CL_2 at 850 K (flux 20 μm, time 480 s). The 2 × 1 nature of the substrate is evident from dimer rows oriented along the diagonal. Chlorine molecules adsorb dissociatively on Si(100) to produce Cl atoms bonded to dangling bonds of Si dimers. While etching is minimal at 300 K, Cl can break dimer bonds at 850 K to form $SiCl_2$, the dominant etch product [2,3]. At 850 K, etching involves Si removal from steps and from terraces. We focus on the latter in this paper. During terrace etching, the dimers are broken, $SiCl_2$ units are liberated, and Si atoms are ejected onto the surface where they can form one-layer high regrowth islands, labeled *I* in Fig. 1. The etch pits have shapes that can be characterized as linear pits (*L*) that are one row wide, linear pits that have a dimer vacancy branch on an adjacent row (*L* + *B*), pits that are two rows wide (*L* + *L*), and so on.

Two distinct mechanisms can be postulated for pit growth. One involves dimer removal adjacent to an existing pit, starting from a dimer vacancy. The other involves creation of isolated dimer vacancies, followed by thermally activated migration and vacancy coalescence. To determine which process is responsible for pit growth in our experiments, we annealed etched surfaces for 2–3 min at 850 K. While continued etching consumed residual surface Cl, analysis showed no significant change

 0031-9007/95/74(11)/2014(4)$06.00

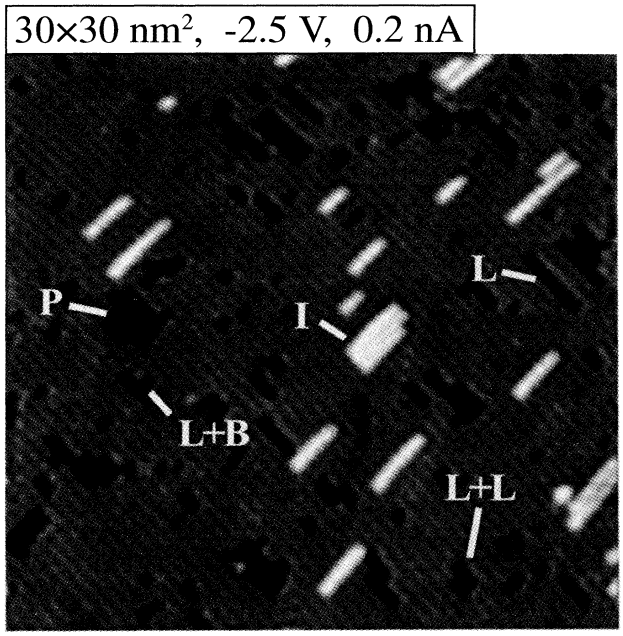

FIG. 1. Occupied-state STM image of Si(100)-(2 × 1) after 9.6 mA s Cl at 850 K (~300 × 300 Å², −2.5 V, and 0.2 nA). Terrace etching produces one-atom-layer deep etch pits, *P*, and Si regrowth islands, *I*. The pits can be characterized based on their shapes, including linear pits (*L*) one row wide, linear pits with one vacancy on the adjacent row (*L* + *B*), and pits that are two rows wide (*L* + *L*).

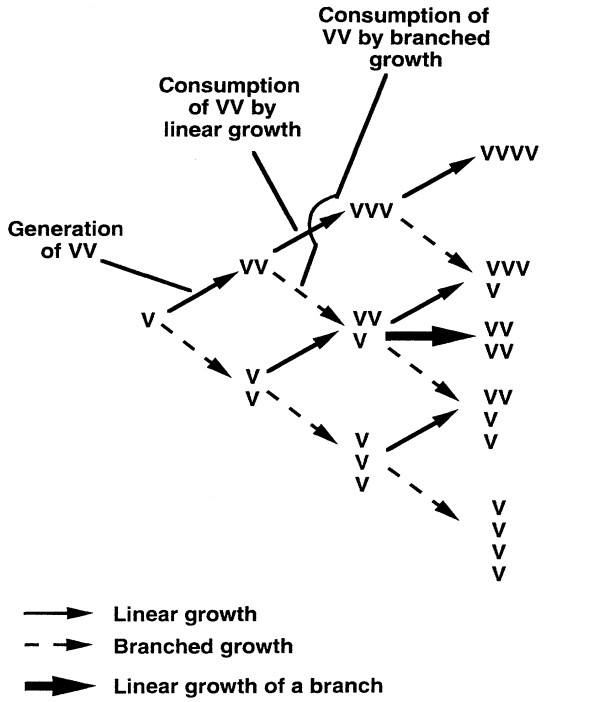

FIG. 2. A schematic depicting growth of etch pits. Competition between pathways leading to pit generation and those that lead to pit consumption governs the areal density of the pits.

in the number densities of pits of various sizes. We conclude that vacancy coalescence does not account for the observed morphology and that pits grow by dimer removal from sites next to existing pits. Reduced vacancy diffusion relative to what has been observed on clean Si(100) can be attributed to the presence of Cl, as for Br-Si(100) where vacancy diffusion was inhibited until complete halogen desorption at ~1100 K (Ref. [7]).

Growth of a single vacancy *V* along a dimer row produces a double linear vacancy *VV*, as depicted in Fig. 2. This unit can continue with linear growth to form *VVV* or a dimer can be removed from the adjacent row to produce a branch. The branched pit can be consumed via linear growth of the major chain, linear growth from the new branch, or branching to form a pit that is three dimers wide. Subsequent growth can be explained in a similar way though the number of channels increases. While etching is exothermic in each case, the population distribution of single layer pits reflects the rates at which new species are generated and consumed. The observed densities of pits with distinct sizes and shapes then result from competition between linear and branching growth.

Pit growth involves distinct steps that can be described by kinetic equations [12] with appropriate rate constants k, including diffusion to a pit edge, activation of a Si atom, diffusion of a second Cl atom to the site, and $SiCl_2$ desorption. There are competing paths that represent Cl diffusion from active sites. Moreover, pit growth requires removal of both atoms of a dimer since single-atom vacancies are not observed. The second atom can be etched in a fashion similar to the first or it can be ejected onto the surface [5]. The ways of removal of the second atom cannot be distinguished, and the rate constant for Si desorption k_D must be considered as an overall rate constant for dimer removal.

Linear pits *L* are produced by the addition of vacancies along the dimer row direction. A single branched growth event along a linear pit produces an *L* + *B* structure. Once formed, the branch can grow along its dimer row direction. Under growth conditions where the probability of linear growth p_L remains constant irrespective of the pit length, the length distribution would follow a decreasing geometrical series distribution or Flory-Schulz distribution [13]; i.e., the number density of pits with i units would be $[V_i] = p_L^{i-1}[V]$, where the brackets indicate areal density and $[V]$ corresponds to a single dimer vacancy. A plot of $\ln([V_i]/[V])$ vs $i - 1$ would confirm this if the slope is a straight line with magnitude $\ln(p_L)$. Physically, p_L denotes the ratio of the linear growth rate to the sum of linear and branching rates for any size. In actuality, one would expect p_L to decrease with length since the rate of branching increases with

length as more sites become available for branching. However, we found that branching occurs preferentially at the chain ends and that this type of branching is dominant for $i < 9$. Thus, the rate of branching and p_L need not change significantly with pit length.

Figure 3 shows $\ln([V_i]/[V])$ vs $i - 1$ for linear pits on Si(100)-(2 × 1) after etching at 850 K. The conditions of Cl fluence and flux were (a) 2 mA s at a flux of 20 μA, (b) 9.6 mA s at 20 μA, and (c) 2 mA s at 10 μA. The slopes of the three lines under a 95% confidence interval give p_L's at 0.68 ± 0.05, 0.69 ± 0.03, and 0.71 ± 0.05, respectively. The constancy of p_L under various conditions of Cl density indicates that we are operating under quasi-steady-state conditions where the parameters governing pit densities are just the rate constants. We conclude that linear pits follow a Flory-Schulz distribution with $p_L = 0.7$. Although energy differences due to rebonding dissimilarities in even- and odd-sized pits have been detected for clean surfaces [14], we observed no dependence of p_L on length that would point to significantly different etching for even and odd pits.

The fact that p_L is a constant for linear growth makes it possible to determine the activation energy difference for linear growth and branch formation. If desorption of $SiCl_2$ is the limiting step in etching, then the probability

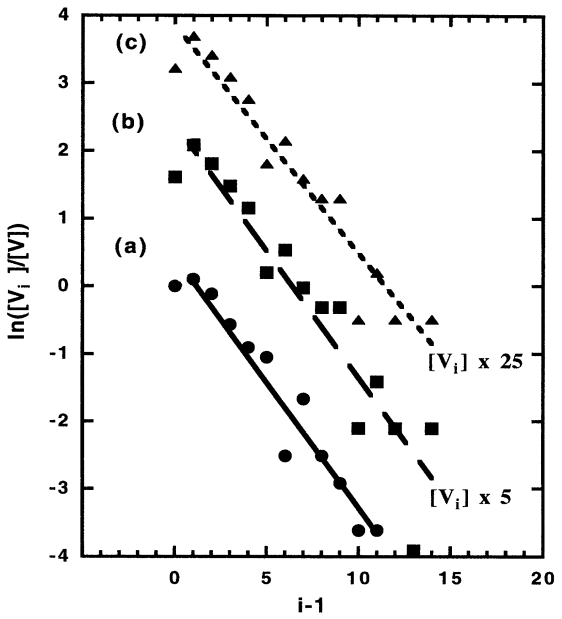

FIG. 3. A plot of size distribution of linear pits observed for Si(100)-(2 × 1) after etching at 850 K with (a) 2 mA s and (b) 9.6 mA s fluence at 20 μA Cl_2 flux and (c) 2 mA s at 10 μA flux. The data are offset for visual clarity. The straight lines indicate the fits using the Flory-Schulz equation with the probability of linear growth $p_L = 0.7 \pm 0.05$. This indicates that the probability of linear growth is almost independent of pit length.

of linear growth can be reduced to

$$p_L = \frac{1}{1 + 2k_{D,B}/k_{D,L}}, \quad (1)$$

where $k_{D,B}$ and $k_{D,L}$ are desorption rate constants for branching and linear growth. In Eq. (1), we have considered that the number of sites available for branching is four, two at each end of a pit, and the number of sites for linear growth is two, one at each end [12]. This is justified since branching is concentrated close to pit ends. Since the distributions of $[V_i]$ in Fig. 3 dictate that p_L is 0.7 ± 0.05, then $k_{D,B}/k_{D,L} = 0.21 \pm 0.05$. The rate constant governing linear growth is then 4.7 ± 1 times that for branch formation.

General rate constants can be written as $k = \sigma \exp(-E/kT)$. We take the prefactors for desorption for linear and branched growth to be the same, an approximation that is reasonable since similar bond-breaking processes are involved in both. Accordingly, $k_{D,B}/k_{D,L} = \exp[-(E_{D,B} - E_{D,L})/kT] = 0.21 \pm 0.05$. The difference in activation energies is then $E_{D,B} - E_{D,L} = 0.11 \pm 0.02$ eV at 850 K. The desorption of a $SiCl_2$ unit from either a branch site or a linear site will involve breaking two Si-Si backbonds and a dimer bond. Hence, the difference in activation energies reflects directional interaction energies between neighboring atoms not forming a dimer. Inspection of the Si surface shows backbonds for atoms adjacent to a pit along the dimer row to be different from those in the next row. In particular, backbonds along the dimer row are for atoms at the pit edge that have three neighbors and a dangling bond, while those on the next row are fully coordinated. The directional interaction energies can be visualized as the energies of step formation. The creation of a branch on a linear pit gives rise to a S_B-type step, whereas the linear growth of the pit leads to an S_A edge, S_A and S_B being the characteristic steps on Si(100). Calculations [14] and measurements [15] predict a formation energy difference of about 0.14 and 0.07 eV, respectively, between S_B and S_A steps. Thus a higher activation barrier for branch creation as compared to linear growth is in accordance with a higher formation energy for the former. This trend between the activation barriers and the formation enthalpies is described very well by the semiempirical Polanyi relationship [16].

Growth of branched pits on the terrace is more complicated than growth of linear pits because the number of channels involved increases with the complexity of the pit shape. The next step in our study corresponds to analysis of growth of linear pits that have one branch, $L + B$. An $L + B$ pit of a given size can be produced by branching from a linear pit or from linear growth of a shorter branched pit (Fig. 2). These pits can be consumed by linear growth, branch creation, and linear growth of the branch. Simple considerations regarding interaction energies between neighboring atoms suggest that linear

growth of a branch adjacent to the parent pit should be faster than growth of the parent pit. Preliminary results indicate that growth of the branch is kinetically favored over growth of the parent by nearly a factor of 2 [12].

Finally, with the activation energies obtained from analysis of terrace etching it is straightforward to model the removal of Si dimers from steps and the step flow process that dominates at lower temperature. Since such etching favors dimer removal along the dimer row direction rather than branching, it should be possible to predict the regularity for etched S_A-type steps and the irregularity for etched S_B-type steps [12].

In this paper, we have considered the etching of Si(100) with Cl, identifying the pathways involved in the formation and growth of pits. We have shown that it is possible to estimate the kinetics and assess the parameters responsible for pit sizes and shapes [9]. Such quantitative analysis based on atomic scale STM images should be applicable to other systems in describing details of surfaces under etching conditions.

This work was supported by Office of Naval Research. We thank D. Rioux, R. J. Pechman, and D. W. Owens for technical assistance and discussion.

*Permanent address: Institute of Materials Science and Technology (INTEMA), Universidad Nacional de Mar del Plata-CONICET, Juan B. Justo 4302, 7600 Mar del Plata, Argentina.

[1] H. F. Winters and J. W. Coburn, Surf. Sci. Rep. **14**, 161 (1992).

[2] R. B. Jackman, H. Ebert, and J. S. Foord, Surf. Sci. **176**, 183 (1986); R. B. Jackman, R. J. Price, and J. S. Foord, Appl. Surf. Sci. **36**, 296 (1989).

[3] Q. Gao, C. C. Cheng, P. J. Chen, W. J. Choyke, and J. T. Yates, Jr., J. Chem. Phys. **98**, 8308 (1993).

[4] F. H. M. Sanders, A. W. Kolfshoten, J. Dieleman, R. A. Haring, A. Haring, and A. E. de Vries, J. Vac. Sci. Technol. A **2**, 487 (1984).

[5] M. Chander, Y. Z. Li, J. C. Patrin, and J. H. Weaver, Phys. Rev. B **47**, 13 035 (1993).

[6] M. Chander, Y. Z. Li, D. Rioux, and J. H. Weaver, Phys. Rev. Lett. **71**, 4154 (1993).

[7] D. Rioux, M. Chander, Y. Z. Li, and J. H. Weaver, Phys. Rev. B **49**, 11 071 (1994).

[8] D. Rioux, R. J. Pechman, M. Chander, and J. H. Weaver, Phys. Rev. B **50**, 4430 (1994).

[9] We restrict ourselves to etching under carefully controlled conditions of halogen flux, surface quality, and temperature. Our conditions are far from those of real etching where the flux can be 10^2–10^3 times greater (as in Ref. [4]) and there can be irradiation by ions, electrons, and photons. Such conditions will introduce more complex reaction pathways than discussed here.

[10] B. S. Swartzentruber, Y.-W. Mo, M. B. Webb, and M. G. Lagally, J. Vac. Sci. Technol. A **7**, 2901 (1989).

[11] M. Chander, Y. Z. Li, J. C. Patrin, and J. H. Weaver, Phys. Rev. B **48**, 2493 (1993).

[12] M. Chander, D. A. Goetsch, C. M. Aldao, and J. H. Weaver (to be published).

[13] See Chaps. 2 and 3 in *Polymer Synthesis,* edited by P. Rempp and E. W. Merrill (Hüthig and Wepf Verlag, New York, 1986); P. J. Flory, Chem. Revs. **39**, 137 (1946).

[14] D. J. Chadi, Phys. Rev. Lett. **39**, 1691 (1987).

[15] B. S. Swartzentruber, Y.-W. Mo, R. Kariotis, M. G. Lagally, and M. B. Webb, Phys. Rev. Lett. **65**, 1913 (1990).

[16] M. Boudart, *Kinetics of Chemical Processes* (Butterworth-Heinemann Reprint Series in Chemical Engineering, Stoneham, MA, 1991).

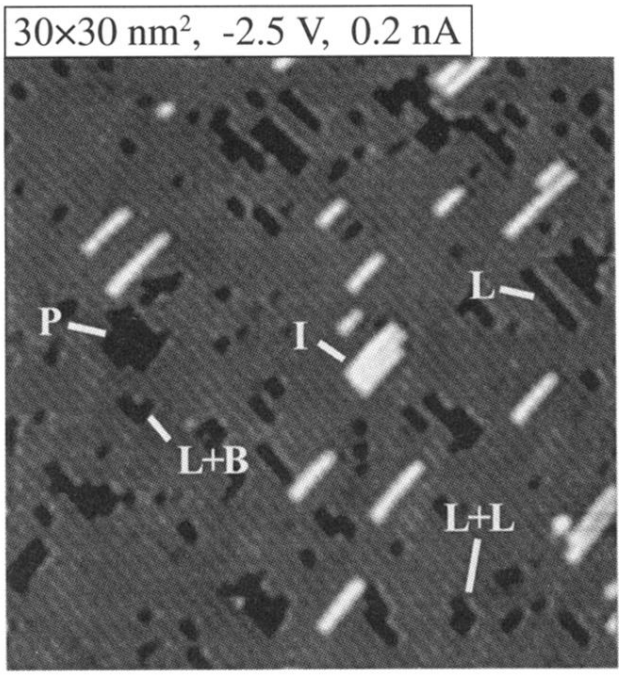

FIG. 1. Occupied-state STM image of Si(100)-(2 × 1) after 9.6 mA s Cl at 850 K (~300 × 300 Å^2, −2.5 V, and 0.2 nA). Terrace etching produces one-atom-layer deep etch pits, *P*, and Si regrowth islands, *I*. The pits can be characterized based on their shapes, including linear pits (*L*) one row wide, linear pits with one vacancy on the adjacent row (*L* + *B*), and pits that are two rows wide (*L* + *L*).